Molecular Mechanisms Underlying KVS-1-MPS-1 Complex Assembly

Yi Wang and Federico Sesti
University of Medicine and Dentistry of New Jersey, Robert Wood Johnson Medical School, Department of Physiology and Biophysics, Piscataway, New Jersey 08854

ABSTRACT Formation of heteromeric complexes between voltage-gated K^+ (Kv) channels and accessory (β) subunits is a widespread means to generate heterogeneity of K^+ current in the nervous system. Here we investigate the principles that determine the interactions of *Caenorhabditis elegans* MPS-1, a bifunctional β-subunit that possesses kinase activity, with Kv channels. MPS-1 belongs to the evolutionarily conserved family of KCNE β-subunits that modulate the functional properties of a variety of Kv channels and that, when defective, can cause congenital and acquired disease in *Homo sapiens*. In Chinese hamster ovary cells, MPS-1 forms stable complexes with different α-subunits. The transmembrane domain of MPS-1 is necessary and sufficient for MPS-1 complex formation. The hydropathicity of the transmembrane domain is an important factor controlling MPS-1 assembly. A highly hydrophobic MPS-1 mutant fails to interact with its endogenous channel partners when transgenically expressed in living worms. The hydropathic mechanism does not require specific points of contact between interacting proteins. This may allow MPS-1 to assemble with various Kv channels, presumably modifying the electrical properties of each.

INTRODUCTION

Voltage-dependent potassium (K^+) channels (Kv) regulate neuronal excitability by controlling the movement of K^+ ions across the membrane in response to changes in the cell voltage. Generally, Kv channels contain additional regulatory proteins or β-subunits that modulate their properties, including permeation, gating, trafficking, location and abundance, sensitivity to stimulation, and pharmacology (1). Thus, β-subunits may represent a widespread means to generate heterogeneity of K^+ current in biological organisms. An example of this process is *Caenorhabditis elegans* MPS-1, a β-subunit that partners with Kv channel KVS-1 to form a complex that is necessary for the normal neuronal function of the animal (2). MPS-1 is a small integral membrane protein with a single transmembrane span. It also possesses a catalytic domain that acts to phosphorylate KVS-1 and other substrates (3). Functional studies have shown that MPS-1 has the ability to control KVS-1 function through independent mechanisms that stem from its β-subunit and protein kinase dual nature (3). Phylogenetically, *mps-1* belongs to the family of *kcne* genes that operate in invertebrates, amphibians, and mammals including *Homo sapiens* (4–7). In humans there are five *kcne* genes; genetic mutations in three of them are linked to congenital and acquired disease (4,8–11). A well-established characteristic of KCNE proteins is the ability to assemble with multiple pore-forming subunits (12,13). This feature makes the study of KCNE proteins particularly significant from a biomedical point of view for the potential impact that a defective *kcne* gene can have on multiple currents (14). MPS-1 is expressed in—and is necessary for the normal function of—neurons where KVS-1 is absent (2). This argues that MPS-1 must partner with several, presently unidentified, Kv channels in the nervous system of *C. elegans*. Thus, the bifunctional nature of MPS-1, together with its putative promiscuous partnering behavior, makes this protein a potentially powerful mediator to generate heterogeneity of neuronal K^+ currents.

The tools available for genetic manipulation of *C. elegans* allow in vivo testing of models elaborated in heterologous expression systems. Toward this end, we use the MPS-1-KVS-1 channel complex as a system to investigate the principles that govern the assembly of MPS-1 with α-subunits. Here we show that the hydropathicity of the transmembrane domain (TMD) of MPS-1 plays an important role in determining its interactions with α-subunits in vivo and in vitro. This domain contains several polar residues that may act to decrease its stability in the cell membrane. We propose a model that predicts that one of the forces driving MPS-1 assembly stems from the need to minimize the electrostatic energy associated with the presence of polar residues embedded in the lipid. Thus, being surrounded by other proteins rather than lipids may increase the stability of MPS-1. This mechanism is consistent with promiscuous assembly of MPS-1 because it would not require specific points of contact between TMDs, a condition almost impossible to fulfill with distinct channels. Thus, simple dielectric forces may allow MPS-1 to generate K^+ current heterogeneity through multiple partnerships by means of both its β-subunit nature and its enzymatic activity.

METHODS AND MATERIALS

Molecular biology

MPS-1 mutants were constructed by polymerase chain reaction (PCR). M1-ΔN was obtained by deleting the first 41 amino acids and by placing a

Submitted April 5, 2007, and accepted for publication June 22, 2007.

Address reprint requests to Federico Sesti, PhD, University of Medicine and Dentistry of New Jersey, Robert Wood Johnson Medical School, Department of Physiology and Biophysics, 675 Hoes Ln., Piscataway, NJ 08854. Tel.: 732-235-4032; Fax: 732-235-5038; E-mail: sestife@umdnj.edu.

Editor: Toshinori Hoshi.

0006-3495/07/11/3083/09 $2.00

doi: 10.1529/biophysj.107.110320

methionine before E42. M1-ΔC was obtained by inserting a stop codon after R70. Thus, M1-ΔN and M1-ΔC had, respectively, three and four residues left before/after the TMD. M1-TM was obtained by placing a methionine before D25 and a stop codon after E94. MPS-1, wild-type, and truncation mutants MPS-3, KVS-1, and human Kv4.2 were epitope tagged in the C-terminus by replacing the terminal stop codon with nucleotides encoding HA residues (YPYDVPDYA-STOP) or c-Myc residues (ISMEQKLISEEDLN). To insert the epitope tags in the N-terminus, a methionine was added in front of the HA or c-Myc sequences, which were fused in frame with the first methionine of MPS-1. The constructs were subcloned into pCI-neo vector (Promega, Madison, WI) for expression in CHO cells. An ~4.5 kb insert of genomic DNA containing the unspliced sequence of *mps-1* and its promoter sequence was inserted into the Fire vector pPD95.75 (1995 Fire Vector Kit) in frame with the *gfp* gene. This construct was used as a template to generate the *mps-1-Q* mutant by PCR. All sequences were confirmed by automated DNA sequencing. Transcripts were quantified with spectroscopy and compared with control samples separated by agarose gel electrophoresis stained with ethidium bromide.

Biochemistry

Immunoprecipitations and coimmunoprecipitations

CHO cells were transiently transfected with cDNA using Superfect kit (Qiagen, Hilden, Germany) and harvested 24–36 h posttransfection. CHO cells were washed with 10 ml ice-cold PBS and lysed with ~2 ml ice-cold RIPA buffer (50 mM TRIS pH 7.4, 150 mM NaCl, 1 mM EDTA, 1% IGEPAL CA-630, 0.5% (w/v) deoxycholate, 0.1% (w/v) SDS, freshly added 10 mM iodoacetamide, phosphatase and protease inhibitors (Calbiochem, San Diego, CA; Roche, Nutley, NJ)) for 30 min at 4°C. Lysates were divided into two equal samples: one for coimmunoprecipitation experiments and one to evaluate total protein expression. Cell lysates were centrifuged for 30 min at 4°C, and the supernatant was mixed with HA-conjugated beads (Roche) and rocked at 4°C for 3 h. Beads were washed three times with RIPA buffer and incubated in SDS sample buffer at ~90–95°C for 10 min. For coimmunoprecipitation, cells were lysed with 1% NP-40 buffer, 50 mM TRIS pH 7.4, 150 mM NaCl, 1 mM EDTA, 1% IGEPAL CA-630, phosphatase and protease inhibitors (Calbiochem). Cell lysates were centrifuged for 60 min at 4°C and the supernatant mixed with HA-conjugated beads (Roche) and rocked at 4°C for 3 hr. Beads were washed three times with ice-cold 1% NP-40 buffer and then incubated in SDS sample buffer at ~90–95°C for 15 min. Visualization was by monoclonal anti-HA (Roche) or anti-c-Myc antibodies from Roche.

Membrane biotinylation

Thirty hours after transfection CHO cells were washed three times with ice-cold PBS, and cell surface proteins were biotinylated by 1.0 mg/ml impermeant biotin analog EZ-link sulfo-NHS-Lcbiotin (Pierce, Rockford, IL) in PBS. After incubation at 4°C for 1 h, cells were washed three times with ice-cold PBS plus 100 mM glycine to remove any remaining biotinylation reagent. Cells were then harvested in RIPA buffer. Lysate proteins were precipitated by (SA)-linked steptoavidin agarose beads and detected by anti-c-Myc antibodies.

Immunocytochemistry

Unpermeabilized cells. Transiently transfected cells were incubated in fresh complete media with anti-HA or anti-c-Myc antibody (40 μg/ml) at 37°C for 1 h. Cells were washed three times with PBS and fixed with paraformaldehyde (4% in PBS) for 15 min at room temperature. After fixing, cells were washed three times for 5 min with PBS and blocked for 1 h at room temperature with 5% nonfat dry milk in PBS plus 0.1% Tween 20. Cells were incubated with the secondary antibody, Cy3-conjugated goat antimouse (Jackson ImmunoResearch, West Grove, PA) (1:2000, in 5% nonfat dry milk in PBS plus 0.1% Tween 20), for 1 h at room temperature and subsequently washed three times for 5 min with PBS.

Permeabilized cells. Transiently transfected cells were washed three times for 5 min with PBS and fixed with paraformaldehyde (4% in PBS) for 15 min at room temperature. After fixing, cells were permeabilized with 0.1% Triton-100X for 5 min at room temperature. Cells were washed with PBS and blocked for 1 h at room temperature with 5% nonfat dry milk in PBS plus 0.1% Tween 20. Cells were incubated in fresh complete media with anti-HA or anti-c-Myc antibody (40 μg/ml) at room temperature for 1 h. Cells were washed with PBS and were incubated with the secondary antibody, Cy3-conjugated goat antimouse, for 1 h at room temperature and subsequently washed three times for 5 min with PBS.

Cells were analyzed with a Zeiss LSM 510 META confocal microscope.

Electrophysiology

Data were recorded with an amplifier, Axopatch 200B (Molecular Devices, Sunnyvale, CA), a PC (Dell, Round Rock, TX), and Clampex software (Axon). Data were filtered at $f_c = 1$ kHz and sampled at 2.5 kHz. Bath solution was (in mM): 4 KCl, 100 NaCl, 10 Hepes (pH = 7.5 with NaOH), 1.8 $CaCl_2$, and 1.0 $MgCl_2$. Pipette solution: 100 KCl, 10 Hepes (pH = 7.5 with KOH), 1.0 $MgCl_2$, 1.0 $CaCl_2$, 10 EGTA (pH = 7.5 with KOH). Whole-cell currents were evoked by 0.1-s voltage sweeps from a holding potential of −80 mV to +120 mV in 20-mV increments.

Construction of transgenic animals expressing wt mps-1 and mps-1-Q

To obtain transgenic nematodes expressing GFP tagged *mps-1* and *mps-1-q*, the reporter constructs were injected with the transformation marker *rol6*(+) and mock DNA into the syncytial gonad of adult hermaphrodite *mps-1 KO* nematodes at the concentration of 20 ng/μl, 50 ng/μl, and 30 ng/μl, respectively. Three transgenic lines carrying extrachromosomal arrays were identified for each construct. Worms were analyzed and photographed with an Olympus BX61 microscope equipped with a digital camera.

RESULTS

To investigate the mechanisms that determine the assembly of MPS-1 with KVS-1, we constructed a succession of MPS-1 truncation mutants (summarized in the *cartoon* in Fig. 1 *A*), cotransfected them with KVS-1 in CHO cells, and evaluated complex formation by coimmunoprecipitation. Protein expression and trafficking to the plasma membrane of the mutants, transfected alone and cotransfected with KVS-1, were also assessed. MPS-1 and KVS-1 were epitope tagged in either the N- (only MPS-1) or C-terminus (both KVS-1 and MPS-1) with the hemagluttinin (HA) and/or the c-Myc epitope tags. Epitope tagging did not alter KVS-1 or MPS-1 functional characteristics (data not shown).

The TMD of MPS-1 mediates assembly with KVS-1

Fig. 1 *B* shows that KVS-1 and wild-type (*wt*) MPS-1 (simply termed MPS-1 if not otherwise stated) coimmunoprecipitated in CHO cells, as expected. MPS-1 could be detected into two separable bands: one running at ~31 kDa (the predicted molecular mass of MPS-1 including the epitope tag) and one running at ~35 kDa. The upper band may reflect

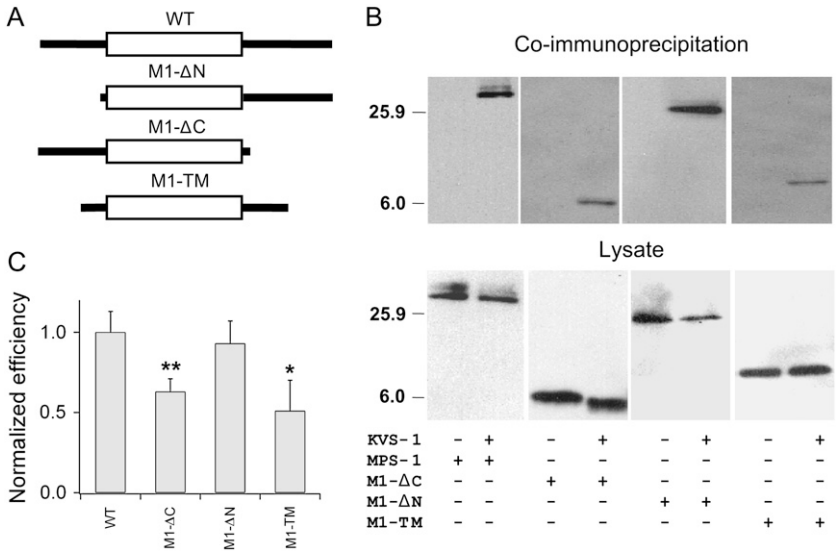

FIGURE 1 The TMD of MPS-1 is necessary and sufficient for KVS-1-MPS-1 complex assembly. (*A*) Cartoon showing the panel of MPS-1 truncation mutants that were generated. (*B*) Coimmunoprecipitations (co-IP) and total protein expression (lysate gels) of KVS-1-HA and MPS-1 or the indicated truncation mutants tagged to the c-Myc epitope tag. Lysates were divided into two equal parts: one for co-IP experiments, one to evaluate protein expression. For co-IP lysates were immunoprecipitated by HA-conjugated beads, separated in SDS PAGE (13.5%), and Western blotted with mouse anti-c-Myc antibody and a horseradish peroxidase chemiluminescence-coupled secondary antibody. For protein expression lysates were Western blotted and visualized by anti-c-Myc antibody as described. (*C*) Densitometry analysis of assembly efficiency of MPS-1 and the indicated mutants. Assembly efficiency was calculated by normalizing band intensity in the co-IP gel to the intensity in the lysate. Data are presented normalized to the assembly efficiency of *wt*. Band intensities were calculated using ImageJ software available at: http://rsb.info.nih.gov/nih-image/Default.html. Number of determinations $n = 4$, 5, 4, and 2, respectively, for *wt*, M1-ΔN, M1-ΔC, and M1-TM. Data are presented as means ± SE. Statistically significant differences from control (ANOVA single-factor) are indicated with, respectively, $*p < 0.03$ and $**p < 0.0001$.

some posttranslational modification such as N-glycosylation (there is a consensus site in the N-terminus) or, alternatively, phosphorylation, possibly self-phosphorylation, and it was not investigated further. We first examined whether the N-terminus of MPS-1 had a role in the mechanisms of interaction. Progressive deletion of the whole domain (M1-ΔN) did not impair the ability of MPS-1 to pair with KVS-1 (Fig. 1 *B*). Similarly, when the whole C-terminus of MPS-1 was deleted (M1-ΔC, Fig. 1 *B*), KVS-1 and the mutant also coimmunoprecipitated (Fig. 1 *B*). The TMD alone (flanked by two extramembranous domains to a final ~10 kDa molecular mass to ensure a minimal cDNA length for protein expression; M1-TM in Fig. 1 *A*) coimmunoprecipitated with KVS-1 (Fig. 1 *B*). Furthermore, disruption of the TMD obtained by inserting a stop codon in its middle gave rise to a proteolytically unstable protein that failed to assemble with KVS-1 or to traffic to the membrane (data not shown). The efficiency of complex formation varied to a considerable extent with different mutants. Densitometry analysis showed that partial or complete deletion of the C-terminus (M1-TM retained about one-third of C-terminal residues) decreased assembly efficiency by ~35% (Fig. 1 *C*).

Normal trafficking of MPS-1 truncation mutants to the plasma membrane

Expression at the plasma membrane of *wt* and truncation mutants, alone or with KVS-1, was assessed by means of membrane biotinylation and immunocytochemistry. Using a membrane-impermeable biotin analog, we found that MPS-1 and the mutant proteins were present at comparable levels in the plasma membrane, suggesting that the deletions did not affect trafficking (Fig. 2 *A*, MPS-1 and the mutants were transfected alone. Controls were performed with tubulin and with unbiotinylated cell transfected with MPS-1) (Fig. 2, *inset*). Epitope tagging in the N-terminus allowed to perform immunocytochemical visualizations without membrane permeabilization. Cells expressing MPS-1 as well the truncation mutants exhibited a characteristic fluorescent ring along the cell boundaries indicating not only that the mutants could reach the plasma membrane normally, in agreement with biotinylation data, but also that their orientation was normal (Fig. 2 *B*. MPS-1 and the mutants were cotransfected with KVS-1). Moreover, cells transfected with mock DNA did not produce any fluorescence (data not shown).

Taken together, these data support the notion that the TMD of MPS-1 is necessary and sufficient for coassembly with KVS-1. The cytoplasmic domain may also contribute but is not necessary. In the following experiments, we focus on the role of the TMD in the mechanisms underlying MPS-1-KVS-1 complex formation.

Complex formation depends on the hydropathicity of the TMD of MPS-1

Close inspection of the sequence of the transmembrane span of MPS-1 (Fig. 3 *A*), the KCNE proteins, and the TMDs of several Kv channels including KVS-1 reveals that, in addition to hydrophobic residues, they contain several polar and/or charged residues. These exert a destabilizing effect on a protein embedded in the membrane because of the low dielectric constant ($\varepsilon \approx 2$) of the lipid. A quantitative measure of the stability of a protein in a lipid membrane is given by the grand average of hydropathicity (GRAVY) coefficient. A large GRAVY coefficient indicates a highly hydrophobic peptide. Table 1 lists GRAVY coefficients calculated

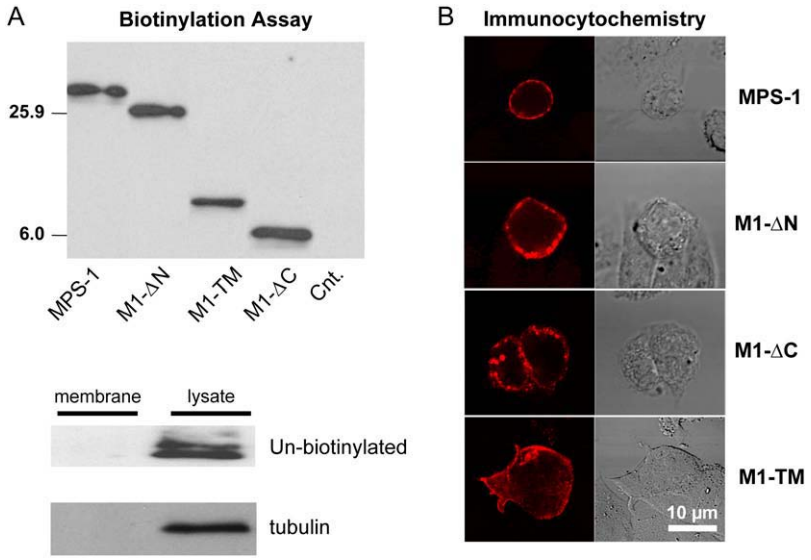

FIGURE 2 Normal trafficking of MPS-1 truncation mutants. (*A*) Surface expression of MPS-1 and the indicated truncation mutants expressed in CHO cells. Mock-transfected cells are indicated with Cnt. Cells were biotinylated with a membrane-impermeant biotin analog and were visualized by a monoclonal antibody to c-Myc. (*Inset*) Controls with tubulin and with unbiotinylated cells transfected with MPS-1. For fluorography, chemiluminescence was performed with a secondary antibody coupled to horseradish peroxidase. (*B*) Immunolocalization of *wt* and the indicated MPS-1 truncation mutants at the cell surface. A c-Myc epitope fused to the N terminus was used for immunolocalization. (*Left*) Immunofluorescence images of unpermeabilized CHO cells transfected with KVS-1 and the indicated MPS-1 variants. (*Right*) Phase-contrast light transmission image of the same fields.

for the TMDs of KVS-1 (named from S1 to S6) and of MPS-1. Human KCNE proteins have GRAVY coefficients that range from 1.735 of KCNE1 to 2.255 of KCNE4. This argues that there must be a functional, as well as a structural, need to accommodate polar/charged residues in the TMDs of these proteins. We hypothesized that the presence of residues acting to lower the stability of the TMD might promote TMD-TMD interactions. The rationale for this idea is that the TMD might increase its stability by being surrounded by other proteins rather than lipids. To test this model, we generated a panel of M1-ΔC mutants in which polar residues were progressively replaced with aliphatic amino acids lacking the polar group but conserving the original three-dimensional structure (serine to alanine and threonine to valine. The tyrosine was mutated to isoleucine; Table 1). Mutation of a single residue (Y47I, T48V, S50A, and S56A) or combinations of two mutations (T48V-S56A, indicated by M1-ΔC-D1 in Fig. 3 *B* and S50A-S56A (not shown)) did not significantly affect the ability of M1-ΔC to assemble with KVS-1. In contrast, mutation of three residues, in different combinations, strongly decreased the efficiency of M1-ΔC-KVS-1 complex formation (Y47I-T48V-S56A or T48V-S50A-S56A, respectively indicated by M1-ΔC-T1 in Fig. 3 *C* and M1-ΔC-T2 (not shown)). As expected, coassembly was not observed when all four polar residues were mutated (M1-ΔC-Q, Fig. 3 *C*). In addition, an M1-ΔC mutant constructed by replacing aliphatic residues in the TMD without significantly altering the GRAVY coefficient (mutation of the ILI triplet to LIL) assembled normally with KVS-1 (data not shown). Biotinylation assays (Fig. 3 *D*) showed that the

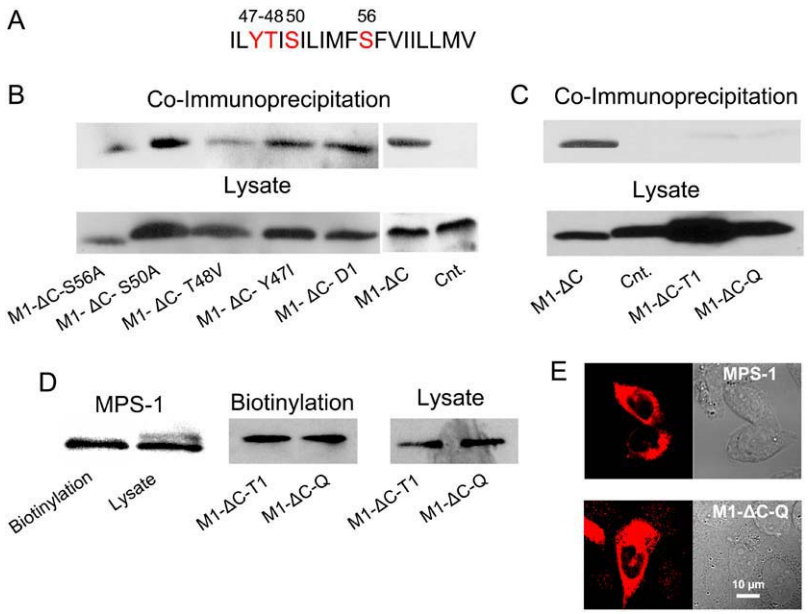

FIGURE 3 Neutralization of polar residues disrupts TMD-TMD interactions. (*A*) Primary sequence of the TMD of MPS-1 with polar residues in red color. (*B*) Coimmunoprecipitation and protein expression of M1-ΔC and the indicated mutants. The control lane (Cnt.) corresponds to CHO cells transfected with M1-ΔC alone. Western blot visualizations as before. (*C*) Coimmunoprecipitation and protein expression of a triple (M1-ΔC-T1, T48V-S50A-S56A) and quadruple (M1-ΔC-Q, Y47I-T48V-S50A-S56A) M1-ΔC mutant. Although the levels of protein expression of the mutants were normal, the mutants failed to coimmunoprecipitate with KVS-1. (*D*) Surface expression of *wt* MPS-1, M1-ΔC-T1, and M1-ΔC-Q mutants (cotransfected with KVS-1) assessed by the means of membrane biotinylation as done before. In all cases the ratio of protein in the biotinylation versus lysate gel is 1:10. (*E*) Cytoplasmic distribution of *wt* MPS-1 and M1-ΔC-Q in permeabilized CHO cells.

TABLE 1 GRAVY coefficients

		MPS-1	
Wt	2.026	T48V-S50A	2.352
Y47I	2.278	S50A-S56A	2.252
T48V	2.239	T48V-S50A-S56A (T2)	2.465
S50A	2.352	Y47I-T48V-S56A (T1)	2.604
S56A	2.139	Y47I-T48V-S50A-S56A (Q)	2.717
		KVS-1	
S1	1.878	S4	1.365
S2	1.292	S5	1.613
S3	1.83	S6	2.261

Secondary structure predictions of membrane proteins were calculated using SOSUI software available at http://bp.nuap.nagoya-u.ac.jp/sosui/sosui_submit.html. Grand average of hydropathicity (GRAVY) coefficients of the TMDs of MPS-1 and KVS-1 were calculated using ProtParam software available at http://www.expasy.org/cgi-bin/protparam.

M1-ΔC mutants exhibited normal levels of expression to the plasma membrane. Thus, the fraction of protein that was detected at the plasma membrane was 11 ± 1% for MPS-1, 13 ± 1% for M1-ΔC (not shown), and 9 ± 1% for M1-ΔC-Q (Fig. 3 *D*, $n = 3$ in all cases) of the total protein (the lysates in the figure were diluted 1:10). Immunocytochemical assays did not reveal any apparent abnormality in the cytoplasmic distribution of the proteins. Thus, replacement of the polar residues in the TMD of M1-ΔC did not give rise to proteolytically unstable proteins that could have failed to coassemble with KVS-1 because of defective trafficking to the plasma membrane, folding, or retention in some intracellular compartment.

Impaired complex formation in hydropathic M1-ΔC mutants

To further test the role of hydropathicity in TMD-TMD interactions and to exclude effects resulting from variable antibody efficiency, we directly compared the ability of MPS-1 and polar mutants to assemble with KVS-1. For this purpose, we used M1-ΔN and M1-ΔC, which by virtue of their different molecular masses could be tagged to the same epitope tag and detected by the same antibody on the same Western blot. Fig. 4 shows that when M1-ΔC and M1-ΔN, which are both tagged to the c-Myc tag in the N-terminus, were cotransfected with KVS-1, they both assembled with the channel. In contrast, when the three polar residues in the transmembrane span of M1-ΔC were mutated (M1-ΔC–T1 in Fig. 4), complex formation was strongly hindered, even though the amount of mutant protein was larger than that of M1-ΔN.

Lowering MPS-3 hydrophobicity increases assembly efficiency

It is interesting to observe that MPS-3 exhibits the lowest number of polar residues in the transmembrane span (a single serine at position 43) and, consequently, MPS-3 has the largest GRAVY coefficient (3.27). Therefore, MPS-3 represented a good tool to test how hydropathicity correlated with coassembly. Notably, MPS-3 coimmunoprecipitated with KVS-1 less efficiently than MPS-1 (Fig. 5. normalized efficiency = 0.35 ± 0.08, $n = 3$). Lowering the hydrophobicity of MPS-3 by introducing a double YT mutation in the corresponding position (F25Y-I26T, GRAVY = 2.7) increased the assembly efficiency of MPS-3 to 0.53 ± 0.04 ($n = 3$) (Fig. 5). Notwithstanding the differences in the secondary structures of the two β-subunits, which may be responsible for their different affinities for KVS-1, these data further strengthen the notion that a decrease in the hydrophobicity of the TMD favors the interaction with KVS-1.

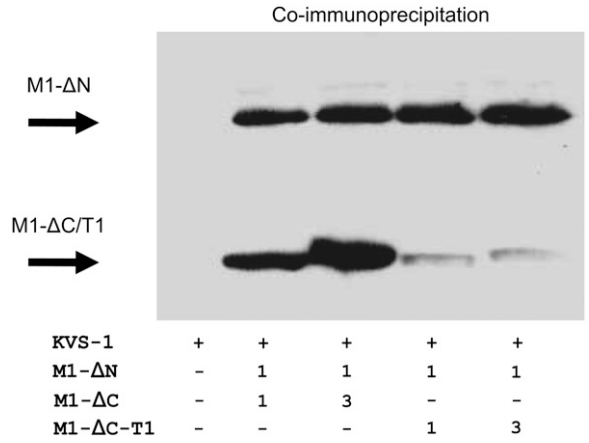

FIGURE 4 M1-ΔC but not M1-ΔC-T1 coimmunoprecipitate with KVS-1. Coimmunoprecipitations of KVS-1 with M1-ΔN and M1-ΔC or M1-ΔN and M1-ΔC-T1. CHO cells were transfected with M1-ΔN and M1-ΔC cDNA in a 1:1 or 1:3 ratio.

M1-ΔC hydropathic mutants do not assemble with human Kv4.2

Physiological partners of MPS-1 other than KVS-1 are presently not identified. Thus, to ascertain if and to what

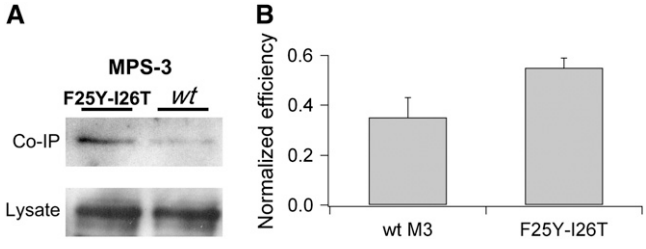

FIGURE 5 Lowering MPS-3 hydrophobicity increases assembly efficiency. (*A*) Representative Western blots of coimmunoprecipitations of *wt* MPS-3 and a F25Y-I26T MPS-3 mutant with KVS-1. (*Bottom*) Total lysates. (*B*) Densitometry analysis of normalized assembly efficiency (to *wt* MPS-1) of *wt* MPS-3 (*wt* M3, $n = 3$) and F25Y-I26T MPS-3 (F25Y-I26T, $n = 3$).

extent the polar mechanism was general or specific to the MPS-1-KVS-1 complex, we employed human Kv4.2, which we showed previously interacts with MPS-1 (2). As expected, *wt* MPS-1 or M1-ΔC coimmunoprecipitated with hKv4.2 (Fig. 6). In contrast, the M1-ΔC-T1 mutant failed to coimmunoprecipitate even though it was abundantly expressed (Fig. 6).

Taken together, these data support two major conclusions. First, the hydropathicity of the TMD is an important factor controlling the assembly of MPS proteins with pore-forming subunits as increasing the GRAVY coefficient decreases assembly efficiency whereas adding polar residues enhances it. Second, the hydropathic mechanism is a general means of interaction that appears to control the interaction of the TMD of MPS-1 with diverse α-subunits.

The hydropathic mechanism controls *wt* MPS-1 interactions

We next estimated the incidence of hydropathic forces in the mechanisms determining the interactions of *wt* MPS-1. Mutation of the four polar residues (M1-Q) decreased the assembly efficiency by more than 50% (Fig. 7, *A* and *B*). To directly compare the ability of *wt* and M1-Q to pair with KVS-1, we coexpressed them in CHO cells and characterized the currents using electrophysiology. Currents expressed in cells that were cotransfected with KVS-1 and M1-Q were indistinguishable from currents in cells transfected with KVS-1 alone (Fig. 7, *C–E*). In contrast, when MPS-1 was added to the cDNA mixture (in a 1:3 ratio with M1-Q), the currents were smaller and inactivated faster, two typical effects of MPS-1 on the current of KVS-1 (Fig. 7, *B–D*) (2).

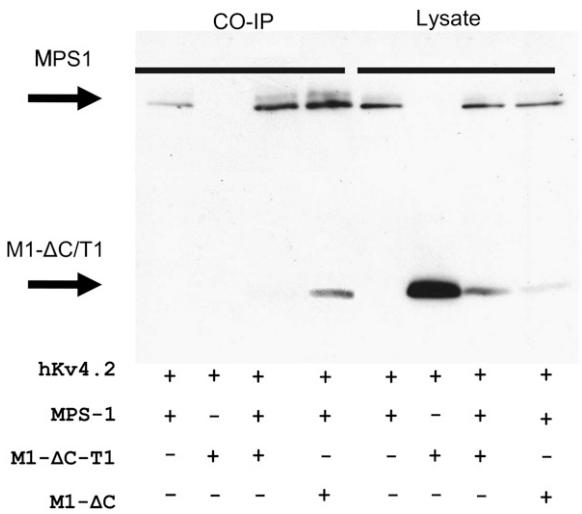

FIGURE 6 M1-ΔC but not M1-ΔC-T1 assembles with human Kv4.2. Coimmunoprecipitations and total lysates of hKv4.2 tagged to the HA epitope tag in the C-terminus with *wt* MPS-1, M1-ΔC, and M1-ΔC-T1. Lysates were immunoprecipitated by HA-conjugated beads and visualized by anti-c-Myc antibody as before.

We have shown previously that, in the native cells, where both MPS-1 and KVS-1 proteins colocalize, the expression/stability of one depends on the other and vice versa (2). To test whether the M1-Q mutant fails to assemble with endogenous KVS-1 in living worms, we constructed transgenic animals expressing *wt* and M1-Q fused to GFP in the C-terminus in an *mps-1* knockout (KO) background. These animals are indicated by, respectively, *VC955*(*wt*) and *VC955*(*m1-q*) in Fig. 7 *F*. As expected, animals expressing *mps-1::gfp* exhibited normal expression (*arrow*). In contrast, the animals expressing *m1-q::gfp* displayed faint fluorescence. Because GFP requires high levels of protein to give detectable signals, these data suggest that the amount of MPS-1 protein at the membrane was decreased in the transgenic animals as a result of impaired complex formation with KVS-1. We conclude that the hydropathic mechanism contributes to MPS-1-KVS-1 complex formation in vivo.

DISCUSSION

Here we investigate the molecular mechanisms governing the assembly of MPS-1 with Kv α-subunits. Biochemical and electrophysiological analyses support the following conclusions. First, MPS-1 can form stable complexes with physiological channel partner KVS-1 and also with evolutionarily distant channels such as human Kv4.2. Second, the TMD is necessary and sufficient for complex formation. The C-terminus can also promote assembly through mechanisms that are poorly understood at present. Third, the hydropathicity of the TMD is a key factor for assembly. Neutralization of polar residues hindered MPS-1's ability to assemble with KVS-1 and hKv4.2. MPS-3, which is the most hydrophobic member in the family, interacted with KVS-1 less efficiently than MPS-1. Notably, the assembly efficiency of MPS-3 could be enhanced by lowering the hydrophobicity of its TMD by mutating the two aliphatic residues FI to YT. It is also interesting to note that MPS-3 cannot form binary complexes with KVS-1 in vivo. However, MPS-3 can partner with KVS-1 when a second MPS protein is present, giving rise to ternary complexes containing two distinct MPS subunits (7). It was imperative for us to ascertain that replacement of multiple polar residues in the transmembrane span of MPS-1 did not give rise to proteotically unstable proteins. The mutants exhibited normal cytoplasmic distribution, trafficking, orientation, and abundance in the plasma membrane. In fact, they partially retained the ability to assemble with the α-subunit.

Polar residues have been shown to promote strong TMD-TMD interactions by establishing hydrogen bonds (15–22). Dawson and colleagues screened a randomized library of transmembrane interfaces and identified two common motifs: SxxSSxxT and SxxxSSxxT (16). Mutations of single serines or threonines in these motifs completely abolished TMD-TMD interactions, indicating that the contact between these positions is very specific. MPS-1 and other KCNE

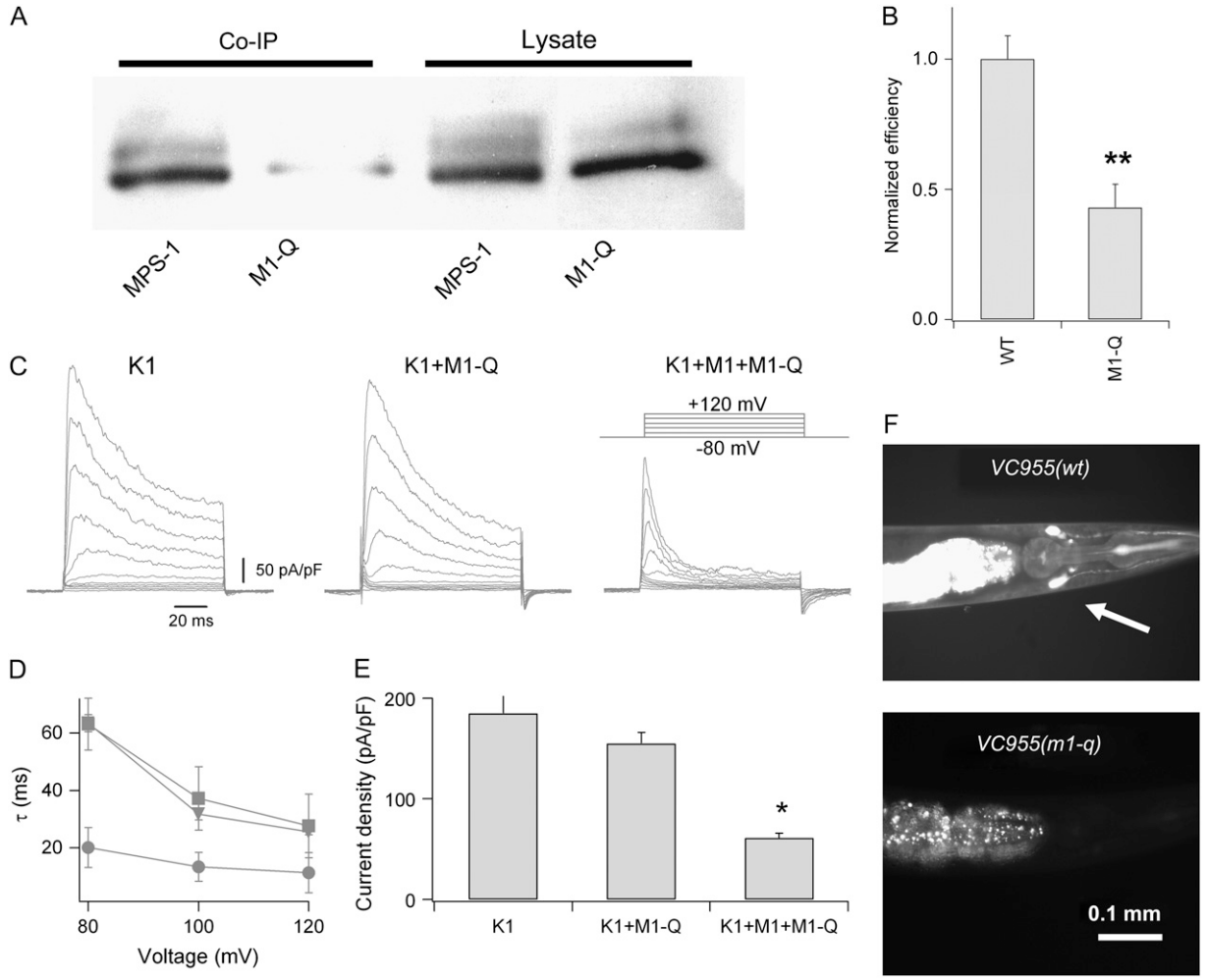

FIGURE 7 Increased hydropathicity in the TMD of *wt* MPS-1 decreases assembly efficiency. (*A*) Coimmunoprecipitations and total lysates of KVS-1 with *wt* MPS-1 or MPS-1-Q (M1-Q). (*B*) Densitometry analysis of assembly efficiency of the mutant ($n = 9$). The symbol ** indicates a statistically significant difference from control ($p < 0.02$). (*C*) Whole-cell currents elicited by voltage jumps from −80 mV to +120 mV in 20-mV increments and 1-s interpulse intervals in cells transfected with KVS-1 alone (KVS-1), M1-Q and KVS-1 (K1+M1-Q), and KVS-1 and MPS-1 and M1-Q in a 1:3 ratio (K1+M1+M1-Q). (*D*) Inactivation rates for currents recorded in cells transfected with KVS-1 alone (*squares*), M1-Q + KVS-1 (*circles*), or MPS-1·+ M1-Q + KVS-1 (*triangles*). Time constants were obtained by fitting macroscopic currents to a single-exponential function: $I_o + I_1\exp(-t/\tau)$. Data are from groups of 10 cells. (*E*) Macroscopic current densities calculated by normalizing the peak current at +120 mV to the cell capacitance in cells transfected with KVS-1 alone, M1-Q + KVS-1, or MPS-1·+ M1-Q + KVS-1. Averages were computed from groups of 10–15 cells. (*F*) Fluorescence microscopy images taken from VC955(*wt*) and VC955(m1-q) transgenic nematode heads. In these focal planes GFP fluorescence (*arrows*) is detectable in amphid neurons. Fluorescence in the intestine is caused by endogenous rhabditin granules. Error bars represent SE. Significant differences from control ($p < 0.05$) are indicated with *.

proteins interact with multiple channels; thus, it would be difficult, if not impossible, to achieve spatial correspondence in these varied conditions. The hydropathicity of the transmembrane span, rather than specific polar residues, may be an important factor for the assembly of MPS-1 with α-subunits. Unlike the peptides considered by Dawson, neutralization of one or two polar residues did not impair the ability of MPS-1 to partner with KVS-1. This suggests two characteristics of MPS-1 interactions with Kv α-subunits. First, spatial correspondence of polar residues is not a requirement. Second, lack of coassembly was not likely caused by structural rearrangements in the TMD because single or double mutations did not hinder pairing. Polar residues exert a destabilizing effect on a protein embedded in the membrane because of the low dielectric constant of the lipid. This argues that there must be a functional as well as a structural need to accommodate these residues. We propose that the need to minimize the electrostatic energy generated by polar residues embedded in the membrane is a primary force behind MPS-1 assembly because surrounding MPS-1 with proteins rather than lipids would decrease the electrostatic energy. This mechanism does not require specific points of contact between TMDs, and as a result, it is consistent with the natural promiscuity of MPS-1 and the other KCNE

proteins. It is also worth considering that ion channels contain several polar/charged residues in their TMDs, which might facilitate MPS-1 incorporation in the complex by the same mechanism.

These data also reveal an unexpected complexity in the mechanisms underlying MPS-1-KVS-1 complex formation. The cytoplasmic domain is a site of interaction—a quantitative estimate shows that this domain can rescue coassembly by 40% when the hydrophilic mechanism is neutralized. Studies with other KCNE proteins point toward a role of this domain in controlling the attributes of such complexes (23–26). This implies that the cytoplasmic domain of KCNE proteins may favor and/or stabilize assembly. The potential role of hydrophobic interactions needs to be elucidated. These are mediated by short-range van der Waals forces (15) that may become particularly effective once the β-subunit is incorporated in the complex. Glycine residues in the transmembrane spans of viral proteins, for instance, are particularly important for fusion activity (27). Thus, the fact that MPS-1 polar mutants and MPS-3 do not assemble efficiently with KVS-1 does not exclude the possibility that van der Waals forces may provide a key contribution to the formation and/or stability of these complexes. The hydropathic mechanism does not explain how structural specificity within the complex is achieved. Functional and biochemical studies indicate that the KCNE proteins occupy specific positions in a complex even though there is controversy as to the specific location (28–32). Further investigations will be needed to address these important issues.

Recently it has been shown that human KCNE1 is retained in the ER and that progression through the secretory pathway requires coassembly with an α-subunit (33,34). On the other hand, several studies have shown that KCNE subunits alone, heterologously expressed in diverse cell lines, can traffic to the plasma membrane (2,35–37). Although in CHO cells MPS-1 alone can traffic to the plasma membrane, in native cells, MPS-1 and other MPS proteins require coassembly with an α-subunit (2,7). Here we confirm this notion by showing that MPS-1-Q mutants do not assemble with KVS-1 in vivo and, as a result, fail to be processed normally. Therefore, the requirement for an α-subunit in heterologous systems remains a matter of controversy.

In summary, we have identified one of the primary mechanisms determining MPS-1-Kv α-subunit assembly. It is highly likely that future studies will elucidate additional aspects of this mechanism, which appears to be remarkably complex, and unravel the mechanisms underlying the assembly of human KCNE genes that we expect will be similar.

The *mps-1* KO strain was a kind gift of the *Caenorhabditis elegans* Knock Out Consortium. We thank Dr. Zui Pan for helping with the confocal microscope, Drs. John Lenard, Shi-Qing Cai, and Noah Weisleder for critical reading of the manuscript, and Laila Sesti for help with the graphics. This work was supported by a National Institutes of Health grant (R01GM68581) to F.S.

REFERENCES

1. Li, Y., S. Y. Um, and T. V. McDonald. 2006. Voltage-gated potassium channels: regulation by accessory subunits. *Neuroscientist.* 12: 199–210.
2. Bianchi, L., S. M. Kwok, M. Driscoll, and F. Sesti. 2003. A potassium channel-MiRP complex controls neurosensory function in *Caenorhabditis elegans*. *J. Biol. Chem.* 278:12415–12424.
3. Cai, S. Q., L. Hernandez, Y. Wang, K. H. Park, and F. Sesti. 2005. MPS-1 is a K^+ channel beta-subunit and a serine/threonine kinase. *Nat. Neurosci.* 8:1503–1509.
4. Abbott, G. W., F. Sesti, I. Splawski, M. E. Buck, M. H. Lehmann, K. W. Timothy, M. T. Keating, and S. A. Goldstein. 1999. MiRP1 forms IKr potassium channels with HERG and is associated with cardiac arrhythmia. *Cell.* 97:175–187.
5. Anantharam, A., A. Lewis, G. Panaghie, E. Gordon, Z. A. McCrossan, D. J. Lerner, and G. W. Abbott. 2003. RNA interference reveals that endogenous *Xenopus* MinK-related peptides govern mammalian K^+ channel function in oocyte expression studies. *J. Biol. Chem.* 278: 11739–11745.
6. Takumi, T., H. Ohkubo, and S. Nakanishi. 1988. Cloning of a membrane protein that induces a slow voltage-gated potassium current. *Science.* 242:1042–1045.
7. Park, K. H., L. Hernandez, S. Q. Cai, Y. Wang, and F. Sesti. 2005. A family of K^+ channel ancillary subunits regulate taste sensitivity in *Caenorhabditis elegans*. *J. Biol. Chem.* 280:21893–21899.
8. Abbott, G., M. H. Butler, S. Bendahhou, M. C. Dalakas, I. J. Ptacek, and S. A. Goldstein. 2001. MiRP2 forms potassium channels in skeletal muscle with Kv3.4 and is associated with periodic paralysis. *Cell.* 104:217–231.
9. Duggal, P., M. R. Vesely, D. Wattanasirichaigoon, J. Villafane, V. Kaushik, and A. H. Beggs. 1998. Mutation of the gene for IsK associated with both Jervell and Lange-Nielsen and Romano-Ward forms of Long-QT syndrome. *Circulation.* 97:142–146.
10. Schulze-Bahr, E., Q. Wang, H. Wedekind, W. Haverkamp, Q. Chen, Y. Sun, C. Rubie, M. Hördt, J. A. Towbin, M. Borggrefe, G. Assmann, X. Qu, J. C. Somberg, G. Breithardt, C. Oberti, and H. Funke. 1997. KCNE1 mutations cause jervell and Lange-Nielsen syndrome. *Nat. Genet.* 17:267–268.
11. Splawski, I., M. Tristani-Firouzi, M. H. Lehmann, M. C. Sanguinetti, and M. T. Keating. 1997. Mutations in the hMinK gene cause long QT syndrome and suppress IKs function. *Nat. Genet.* 17:338–340.
12. McCrossan, Z. A., and G. W. Abbott. 2004. The MinK-related peptides. *Neuropharmacology.* 47:787–821.
13. Cai, S. Q., K. H. Park, and F. Sesti. 2006. An evolutionarily conserved family of accessory subunits of K^+ channels. *Cell Biochem. Biophys.* 46:91–100.
14. Abbott, G. W., and S. A. Goldstein. 2002. Disease-associated mutations in KCNE potassium channel subunits (MiRPs) reveal promiscuous disruption of multiple currents and conservation of mechanism. *FASEB J.* 16:390–400.
15. Curran, A. R., and D. M. Engelman. 2003. Sequence motifs, polar interactions and conformational changes in helical membrane proteins. *Curr. Opin. Struct. Biol.* 13:412–417.
16. Dawson, J. P., J. S. Weinger, and D. M. Engelman. 2002. Motifs of serine and threonine can drive association of transmembrane helices. *J. Mol. Biol.* 316:799–805.
17. Dawson, J. P., R. A. Melnyk, C. M. Deber, and D. M. Engelman. 2003. Sequence context strongly modulates association of polar residues in transmembrane helices. *J. Mol. Biol.* 331:255–262.
18. Feng, J., M. E. Call, and K. W. Wucherpfennig. 2006. The assembly of diverse immune receptors is focused on a polar membrane-embedded interaction site. *PLoS Biol.* 4:e142.
19. Garrity, D., M. E. Call, J. Feng, and K. W. Wucherpfennig. 2005. The activating NKG2D receptor assembles in the membrane with two signaling dimers into a hexameric structure. *Proc. Natl. Acad. Sci. USA.* 102:7641–7646.

20. Adamian, L., and J. Liang. 2002. Interhelical hydrogen bonds and spatial motifs in membrane proteins: polar clamps and serine zippers. *Proteins*. 47:209–218.

21. Adamian, L., and J. Liang. 2001. Helix-helix packing and interfacial pairwise interactions of residues in membrane proteins. *J. Mol. Biol.* 311:891–907.

22. Gratkowski, H., J. D. Lear, and W. F. DeGrado. 2001. Polar side chains drive the association of model transmembrane peptides. *Proc. Natl. Acad. Sci. USA*. 98:880–885.

23. Gage, S., and W. Kobertz. 2004. KCNE3 truncation mutants reveal a bipartite modulation of KCNQ1 K^+ channels. *J. Gen. Physiol.* 124: 759–771.

24. Melman, Y. F., A. Krumerman, and T. V. McDonald. 2002. A single transmembrane site in the KCNE-encoded proteins controls the specificity of KvLQT1 channel gating. *J. Biol. Chem.* 277:25187–25194.

25. Melman, Y. F., A. Domenech, S. de la Luna, and T. V. McDonald. 2001. Structural determinants of KvLQT1 control by the KCNE family of proteins. *J. Biol. Chem.* 276:6439–6444.

26. Abbott, G. W., M. H. Butler, and S. A. Goldstein. 2006. Phosphorylation and protonation of neighboring MiRP2 sites: function and pathophysiology of MiRP2-Kv3.4 potassium channels in periodic paralysis. *FASEB J*. 20:293–301.

27. Cleverley, D. Z., and J. Lenard. 1998. The transmembrane domain in viral fusion: essential role for a conserved glycine residue in vesicular stomatitis virus G protein. *Proc. Natl. Acad. Sci. USA*. 95:3425–3430.

28. Melman, Y. F., S. Y. Um, A. Krumerman, A. Kagan, and T. V. McDonald. 2004. KCNE1 binds to the KCNQ1 pore to regulate potassium channel activity. *Neuron*. 42:927–937.

29. Tai, K., and S. Goldstein. 1998. The conduction pore of a cardiac potassium channel. *Nature*. 391:605–608.

30. Kurokawa, J., H. Motoike, and R. Kass. 2001. TEA(+)-sensitive KCNQ1 constructs reveal pore-independent access to KCNE1 in assembled I(Ks) channels. *J. Gen. Physiol.* 117:43–52.

31. Chen, H., F. Sesti, and S. A. Goldstein. 2003. Pore- and state-dependent cadmium block of I(Ks) channels formed with MinK-55C and wild-type KCNQ1 subunits. *Biophys. J*. 84:3679–3689.

32. Tapper, A., and A. J. George. 2000. MinK subdomains that mediate modulation of and association with KvLQT1. *J. Gen. Physiol.* 116: 379–390.

33. Chandrasekhar, K. D., T. Bas, and W. R. Kobertz. 2006. KCNE1 subunits require co-assembly with K(+) channels for efficient trafficking and cell surface expression. *J. Biol. Chem.* 281:40015–40023.

34. McCrossan, Z. A., A. Lewis, G. Panaghie, P. N. Jordan, D. J. Christini, D. J. Lerner, and G. W. Abbott. 2003. MinK-related peptide 2 modulates Kv2.1 and Kv3.1 potassium channels in mammalian brain. *J. Neurosci.* 23:8077–8091.

35. Bianchi, L., Z. Shen, A. T. Dennis, S. G. Priori, C. Napolitano, E. Ronchetti, R. Bryskin, P. J. Schwartz, and A. M. Brown. 1999. Cellular dysfunction of LQT5-MinK mutants: abnormalities of IKs, IKr and trafficking in long QT syndrome. *Hum. Mol. Genet*. 8:1499–1507.

36. Krumerman, A., X. Gao, J. S. Bian, Y. F. Melman, A. Kagan, and T. V. McDonald. 2004. An LQT mutant minK alters KvLQT1 trafficking. *Am. J. Physiol. Cell Physiol*. 286:C1453–1463.

37. Grunnet, M., T. Jespersen, H. B. Rasmussen, T. Ljungstrøm, N. K. Jorgensen, S. P. Olesen, and D. A. Klaerke. 2002. KCNE4 is an inhibitory subunit to the KCNQ1 channel. *J. Physiol.* 542:119–130.